

Energy Efficiency Analysis of 5G Ultra-dense Networks Based on Random Way Point Mobility Models

Junliang Ye¹, Yuanyuan He¹, Xiaohu Ge¹, Min Chen²

¹School of Electronic Information and Communications

Huazhong University of Science and Technology, Wuhan 430074, Hubei, P. R. China.

²School of Computer Science and Technology

Huazhong University of Science and Technology, Wuhan 430074, Hubei, P. R. China.

Corresponding author: Xiaohu Ge

Abstract—With ultra-dense networks (UDN) becoming one of the key technologies of the fifth generation (5G) cellular networks, it is an important problem to evaluate the influence of user mobility on UDN. However, studies that focus on this topic are still not enough. In this paper, random way point mobility models and the stochastic geometry theory are considered to evaluate the performance of 5G UDN. We first derive the coverage probability of UDN for macro-cell users and small-cell users based on random small cell networks. Furthermore, the network capacity and energy efficiency are evaluated for UDN considering user mobility, respectively. Compared with the existed studies, we provide a new kind of method to study the impact of user mobility for the future 5G UDN.

Index Terms—User mobility, ultra-dense networks, 5G networks, random way point model.

I. INTRODUCTION

Recently, technologies of wireless cellular network have been improved dramatically and successfully influenced our lives in many aspects. Nowadays the 5G networks require 1000 times of the transmission rate compared with past cellular network systems. To overcome the challenge researchers start to consider the Ultra dense networks (UDN) should be one of the key technologies to fit the demand of huge transmission rate [1]. The UDN are mainly used to reduce the coverage area of one single small cell base station (SBS) and further improve the performance of the whole networks [2]. On the other hand, the effect of user mobility is enlarged because of the decline of the cell radius. Thus, it is an important problem to evaluate the impact of the user mobility for 5G small cell networks considering human activity habits [3].

From UDN first introduced till now, many kinds of works have been done over this topic. The authors of [4] pointed out that the UDN would be the main component of future networks and gave us a brief answer of a basic question: how many SBS do we need to build a 5G cellular system? The influence of SBS density on network energy efficiency (EE) has also been studied in [5] using stochastic geometry theory. Some researchers focus on the combination of 5G key technologies, reference [6] provided a framework to use Massive-MIMO and mmWave for UDN backhaul transmission. MmWave was also considered in [7] to study the coverage probability in UDN

with different network parameters. The authors of [8] found that the differences between line of sight (LoS) and non-LoS transmission would cause a crucial impact in UDN theoretic models. There are also some researchers think that the way to design the networks should be evolved in UDN designing, like the authors of [9] introduced a concept of user-centric UDN aim at using dynamic AP grouping technology to realize allocating network resources more intelligently. Traditional WIFI technologies were studied as a component of UDN in [10] to establish a LTE-WIFI small-cell dense network, and multi dimension Markov chain was used to study the network performance in that paper. Other well-known technologies could also be used in UDN like [11] gave us a joint research between cognitive radio and USDN to study the impact of different resource allocation algorithms on UDN. Cooperative communication is similarly considered as a necessary part of UDN, [12] has done a joint optimization between spectral efficiency and EE of UDN using cooperative game theory. Also some new technologies can be used in UDN, like energy harvesting, reference [13] predicted there would be a trade-off between EE and coverage probability if we adopt energy harvesting devices in UDN.

From 5G standard was first introduced till now, so many researches are focus on different topics of UDN, but the impact of user mobility in UDN is still not well studied. Based on this fact, the contributions and novelties of this paper are summarized as follow:

- 1) Providing a way to evaluate user mobility in UDN by utilizing the well-known Random way point (RWP) mobility model together with stochastic geometry model.
- 2) Based on the proposed RWP model, we analyze the network performance indexes like network capacity and EE.

The rest of this paper is organized as follow. Section two describes the system model of a downlink UDN with users mobility follow RWP. In section three the network performance indexes like coverage probability, network capacity and EE are derived based on the proposed system model. Numerical and simulation results are shown in section four. Finally, section five concludes this paper.

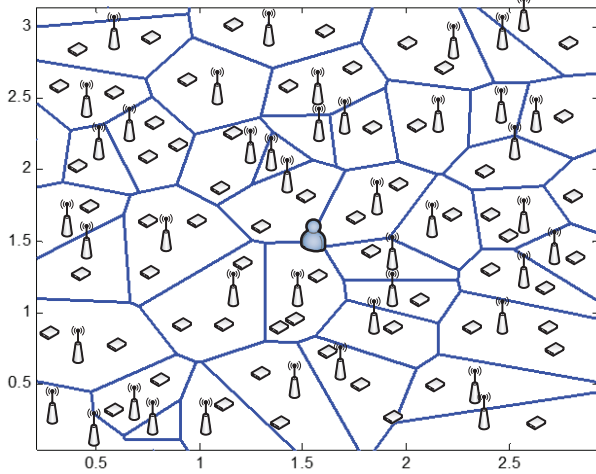


Fig. 1. System model. A PVT network including MBS, SBS and one TU inside.

II. SYSTEM MODEL

A. Base Stations Distribution Model

Assume that both macro cell base stations (MBS) and small cell base stations (SBS) are located on the two dimension plane \mathbb{R}^2 . The distribution processes of MBS and SBS follow two independent homogeneous Poisson point processes (HPPP) Φ_m and Φ_s with intensity λ_{B_m} and λ_{B_s} , respectively. Consider the fact that the density of SBS is always larger than that of MBS in a real cellular system, we assume that $\lambda_{B_s} > \lambda_{B_m}$. Using Poisson-Voronoi Tessellation (PVT) on Φ_m the plane is partitioned into a series of irregular polygons that corresponding to different MBS coverage areas [14]. MBS and SBS are assumed to transmit signal on different and disjoint spectrums so that there is no cross tier interference in our proposed UDN system. The users are uniformly and independently located on the plane with intensity λ_u , so based on the Slivnyaks theory, we can choose any one of the users as the typical user (TU) to study and extend the analyze results to all other users without loss of generality. An illustration of users and BSs deployment is depicted in Fig. 1.

B. Interference Model

Assume that the user devices and base stations are all equipped with single antenna, and the multiple access technology is OFDM. Because of the usage of OFDM technology, there is no inter cell interference in our network model, and the downlink interference come from other base stations on the plane. The user mobility is evaluated by RWP model [15] and explained in part C of this section. Due to the large density of SBS we make the same assumption as [3] that the moving users can only access the MBS and static users can access the SBS in order to decrease the huge overhead caused by cross cell movements. Because of the usage of PVT method, TU will choose the closest base station to access, and TU can successfully served only if the received signal-to-interference-plus-noise ratio (SINR) of the downlink channel is beyond a given threshold T .

The wireless channel is assumed to be Rayleigh fading channel in this paper. Denote the transmit power of MBS and SBS is p_m and p_s , respectively. According to the different and disjoint working spectrum between MBS and SBS, the users of MBS/SBS can only receive interference from other MBS/SBS. So when the MBS b_{m_0} try to cover a moving TU, the received interference of TU can be expressed as:

$$I_{rm} = \sum_{i \in \Phi_m / b_{m_0}} p_m h_{i_m} R_{i_m}^{-\alpha} \quad , \quad (1)$$

where R_{i_m} is the distance between interfering MBS and TU, h_{i_m} is an exponential random variable with expectation equals to 1, α represents the path loss exponent.

And received interference of the downlink channel between a static TU and its associated SBS b_{s_0} is:

$$I_{rs} = \sum_{i \in \Phi_s / b_{s_0}} p_s h_{i_s} R_{i_s}^{-\alpha} \quad , \quad (2)$$

where R_{i_s} denotes the distance between interfering SBS and TU.

C. User Mobility Model

The RWP model is used to evaluate the mobility of users in this paper. In RWP model, users have two kinds of states, one is moving and the other is static. A TU will keep static for a certain waiting time t_p , and when t_p is ended the TU will straightly move to a random destination ue_d which is uniformly distributed on the plane. The moving velocity $v(n)$ of this movement is choosing from $[\min velocity, \max velocity]$ uniformly, where n denotes the total number of movements before. Notice when TU starts one movement, the velocity will keep constant before the ending of this movement. We use $t_m(n)$ to denote the duration of the n th movement, and $ue_x(n)$, $ue_y(n)$ denote the x-coordinate and y-coordinate of the destinations location of the n th movement. Also define the distance between $n-1$ th destination and n th destination as $d(n)$, the angel between them is $\theta(n)$, then we have:

$$\begin{cases} d(n) = \sqrt{(ue_x(n) - ue_x(n-1))^2 + (ue_y(n) - ue_y(n-1))^2} \\ t_m(n) = \frac{d(n)}{v(n)} \\ \sin \theta(n) = \frac{ue_y(n) - ue_y(n-1)}{d(n)} \\ \cos \theta(n) = \frac{ue_x(n) - ue_x(n-1)}{d(n)} \end{cases} \quad (3)$$

And once the TU finishes a movement, he will keep static for another t_p again.

III. PERFORMANCE ANALYSIS

A. Coverage Probability

The definition of coverage probability is shown as follow [16]:

$$p_c(T, \lambda, \alpha) \triangleq P[SINR > T] \quad , \quad (4)$$

where λ is the density of the base stations.

Due to the assumption that the MBS and SBS use different and disjoint spectrums, so there is no cross tier interference in the whole networks. Thus the coverage probability of MBS and SBS are independent with each other. By denoting σ^2 as the variance of the normal distributed additive Gaussian white noise, p as the transmit power of the base station, r as the distance between the associated base station and user, h as the small scale fading of the wireless channel, if h is an exponential distributed variable, the coverage probability can be expressed as follow:

$$p_c(T, \lambda, \alpha) = \pi\lambda \int_0^\infty e^{-\pi\lambda v(1+\rho(T,\alpha))-\mu T\sigma^2 v^{\alpha/2}} dv, \quad (5)$$

where:

$$\rho(T, \alpha) = T^{2/\alpha} \int_{T^{-2/\alpha}}^\infty \frac{1}{1+u^{\alpha/2}} du, \quad (6)$$

with $u = \left(\frac{v}{rT\frac{\alpha}{\sigma}}\right)^2$. And notice that in our model the users can be successfully covered if and only if the received SINR between the moving users and the associated MBS are beyond T , or the received SINR between the static users and the associated SBS are beyond T . So by denoting $p_{m_c}(T, \lambda, \alpha)$ and $p_{s_c}(T, \lambda, \alpha)$ as the coverage probability of moving and static users respectively, when $\alpha = 4$ formula (6) can be further derived as (7)(8) and (9).

B. Network Capacity

According to the famous Shannon formula $C = B \cdot \log_2(1 + SINR)$, where C is the channel capacity and B is the single channel bandwidth, the stationary channel capacity of TU can be expressed by:

$$\overline{C_u} = \lim_{t \rightarrow \infty} \frac{\mathbb{E}(C_s)t_s + \mathbb{E}(C_m)t_m}{t}, \quad (10)$$

where $\mathbb{E}(C_s)$ and $\mathbb{E}(C_m)$ are the expectation channel capacity of SBS and MBS, t_s and t_m denote the total time that SBS and MBS can cover the TU, respectively. Notice that there exists the situation that user cannot be covered because of the poor received SINR, so we have $t_m + t_s \leq t$.

Together with formula (8), $\mathbb{E}(C_s)$ and $\mathbb{E}(C_m)$ can be expressed as (11)(12):

Where $\rho(x, \alpha)$ has been shown in (6).

Thus substitute (5) (6) into (10), the total network capacity is expressed as (13):

Where S represents the area of the plane, t_s and t_m are achieved through Monte-Carlo simulation.

C. Energy Efficiency

In this paper, the EE is defined as follow:

$$\varpi = \frac{\overline{C_{total}}}{E}, \quad (14)$$

where ϖ is the network EE, $\overline{C_{total}}$ is the total network capacity, E stands for the total energy consumption.

In our model, four kinds of energy consumption is considered, the first is MBS transmit energy consumption

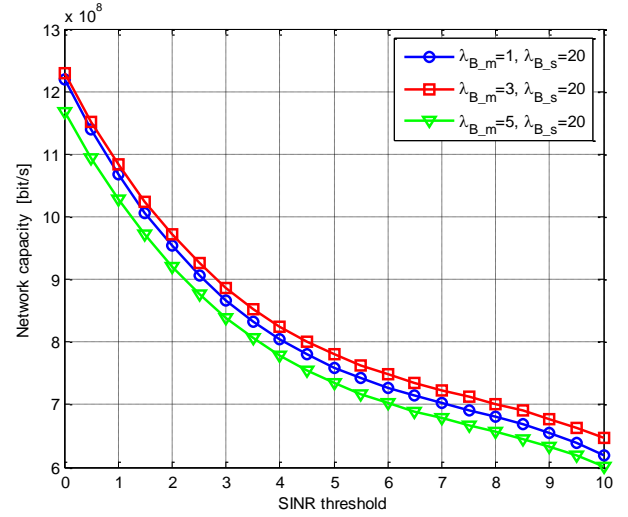


Fig. 2. Network capacity with respect to MBS density and SINR threshold.

$P_{m_trans} = p_m \lambda_u S p_{m_c}(T, \lambda_{B_m}, \alpha)$, second is SBS transmit energy consumption $P_{s_trans} = p_s \lambda_u S p_{s_c}(T, \lambda_{B_s}, \alpha)$, third is MBS operating energy consumption $P_{m_opr} = a P_{m_trans} + b_m$, the final one is SBS operating energy consumption $P_{s_opr} = a P_{s_trans} + b_s$ with $a = 7.84$, $b_m = 71.50$ W for MBS and $a = 7.84$, $b_s = 7.15$ W for SBS. So the network energy efficiency can be evaluated as (15):

IV. SIMULATION RESULTS

This section is about the Monte-Carlo simulation results of our proposed model. The simulation parameters are defined as follow: $S = \sqrt{10} \times \sqrt{10}$ km², $\lambda_u = 500$ per square kilometer, transmit power of SBS and MBS are $p_s = 0.05$ W and $p_m = 0.1$ W, path loss exponent $\alpha = 4$, variance of Gaussian noise $\sigma^2 = 0.001$ and the bandwidth of one single channel $B = 100$ KHz. For the parameters in RWP model, we set the waiting time $t_p = 240$ min, and moving velocity are uniformly and randomly picked in $[0.22, 1]$ km/min.

Fig. 2 shows the network capacity $\overline{C_{total}}$ with respect to the MBS density λ_{B_m} and SINR threshold T . An interesting observation is that when the SINR threshold is fixed, the network capacity λ_{B_m} does not monotone increase with the MBS density. As we can see in the figure, when $\lambda_{B_m} = 3$ the corresponding $\overline{C_{total}}$ is larger than those of $\lambda_{B_m} = 5$ and $\lambda_{B_m} = 1$, and this result can also be seen in [4]. On the other hand, the network capacity decreases with the increase of SINR threshold, it's similar to the well-known result in [14], [16].

In Fig.3 the influence of SBS density λ_{B_s} and SINR threshold T on the network capacity $\overline{C_{total}}$ is evaluated. As the SINR threshold is fixed, we can see that the network capacity decreases with the increase of SBS density λ_{B_s} . And if the SBS density is fixed the $\overline{C_{total}}$ decreases with the increase of SINR threshold T .

The effect of MBS density λ_{B_m} and SINR threshold T on the network energy efficiency ϖ is investigated in Fig. 4. We can see from the figure that when T is fixed, among

$$p_{m_c}(T, \lambda, 4) = \frac{\pi^{\frac{3}{2}}}{\sqrt{\frac{T}{SNR_m}}} \exp\left(\frac{(\lambda_{B_m} \pi \kappa(T))^2}{\frac{4T}{SNR_m}}\right) Q\left(\frac{\lambda_{B_m} \pi \kappa(T)}{\sqrt{\frac{2T}{SNR_m}}}\right), \quad (7)$$

$$p_{s_c}(T, \lambda, 4) = \frac{\pi^{\frac{3}{2}}}{\sqrt{\frac{T}{SNR_s}}} \exp\left(\frac{(\lambda_{B_s} \pi \kappa(T))^2}{\frac{4T}{SNR_s}}\right) Q\left(\frac{\lambda_{B_s} \pi \kappa(T)}{\sqrt{\frac{2T}{SNR_s}}}\right), \quad (8)$$

$$\kappa(T) = 1 + \rho(T, 4) = 1 + \sqrt{T}(\pi/2 - \arctan(1/\sqrt{T})) \quad , \quad (9a)$$

$$Q(x) = \frac{1}{\sqrt{2\pi}} \int_x^\infty \exp(-y^2/2) dy \quad , \quad (9b)$$

$$SNR_m = \frac{p_m}{\mu\sigma^2} \quad , \quad (9c)$$

$$SNR_s = \frac{p_s}{\mu\sigma^2} \quad . \quad (9d)$$

$$\mathbb{E}(C_s) = \int_0^\infty \log_2(1+x) \left(-x \frac{d\left(\pi(\lambda_{B_s}) \int_0^\infty e^{-\pi(\lambda_{B_s})v(1+\rho(x,\alpha))-\mu x\sigma^2 v^{\alpha/2}} dv\right)}{dx} \right) dx \quad . \quad (11)$$

$$\mathbb{E}(C_m) = \int_0^\infty \log_2(1+x) \left(-x \frac{d\left(\pi(\lambda_{B_m}) \int_0^\infty e^{-\pi(\lambda_{B_m})v(1+\rho(x,\alpha))-\mu x\sigma^2 v^{\alpha/2}} dv\right)}{dx} \right) dx \quad . \quad (12)$$

$$\begin{aligned} \overline{C_{total}} &= S\lambda_u \overline{C_u} \\ &= S\lambda_u \lim_{t \rightarrow \infty} \frac{\mathbb{E}(C_s)t_s + \mathbb{E}(C_m)t_m}{t} \\ &= \lim_{t \rightarrow \infty} \frac{S\lambda_u t_s \int_0^\infty \log_2(1+x) \left(-x \frac{d\left(\pi(\lambda_{B_s}) \int_0^\infty e^{-\pi(\lambda_{B_s})v(1+\rho(x,\alpha))-\mu x\sigma^2 v^{\alpha/2}} dv\right)}{dx} \right) dx}{t} + \\ &\quad \lim_{t \rightarrow \infty} \frac{S\lambda_u t_m \int_0^\infty \log_2(1+x) \left(-x \frac{d\left(\pi(\lambda_{B_m}) \int_0^\infty e^{-\pi(\lambda_{B_m})v(1+\rho(x,\alpha))-\mu x\sigma^2 v^{\alpha/2}} dv\right)}{dx} \right) dx}{t} \quad . \end{aligned} \quad (13)$$

$$\begin{aligned} \varpi &= \lim_{t \rightarrow \infty} \frac{S\lambda_u t_s \int_0^\infty \log_2(1+x) \left(-x \frac{d\left(\pi(\lambda_{B_s}) \int_0^\infty e^{-\pi(\lambda_{B_s})v(1+\rho(x,\alpha))-\mu x\sigma^2 v^{\alpha/2}} dv\right)}{dx} \right) dx}{(P_{m_trans} + P_{s_trans} + P_{m_opr} + P_{s_opr})t} + \\ &\quad \lim_{t \rightarrow \infty} \frac{S\lambda_u t_m \int_0^\infty \log_2(1+x) \left(-x \frac{d\left(\pi(\lambda_{B_m}) \int_0^\infty e^{-\pi(\lambda_{B_m})v(1+\rho(x,\alpha))-\mu x\sigma^2 v^{\alpha/2}} dv\right)}{dx} \right) dx}{(P_{m_trans} + P_{s_trans} + P_{m_opr} + P_{s_opr})t} \quad . \end{aligned} \quad (15)$$

all the three couples of parameters $\lambda_{B_m} = 3$ achieves the largest energy efficiency, and when the MBS density is fixed, the energy efficiency decreases with the increase of SINR threshold T .

Finally, the impact of SBS density λ_{B_s} and SINR threshold T for the network energy efficiency ϖ is shown in Fig. 5. The simulation result shows that when T is fixed, energy efficiency ϖ decreases with the increase of λ_{B_s} . Similarly, when λ_{B_s} is fixed, energy efficiency ϖ decreases with the increase of

SINR threshold T .

V. CONCLUSION

Based on the RWP model and stochastic geometry theory, the impact of user mobility performance on 5G UDN is studied in this paper. The simulation results indicate that when we take user mobility into consideration, the network capacity still does not monotone increase with base station density. This paper has established a brief but effective way to evaluate the

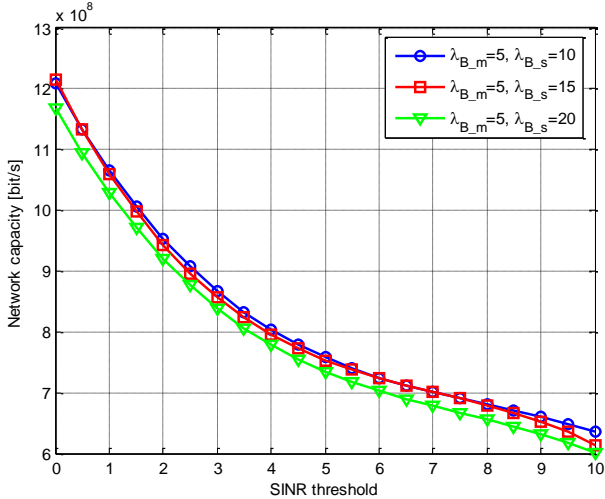


Fig. 3. Network capacity with respect to SBS density and SINR threshold.

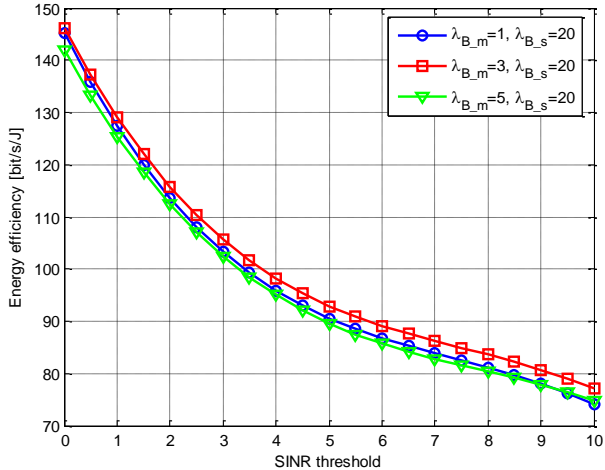


Fig. 4. Energy efficiency with respect to MBS density and SINR threshold.

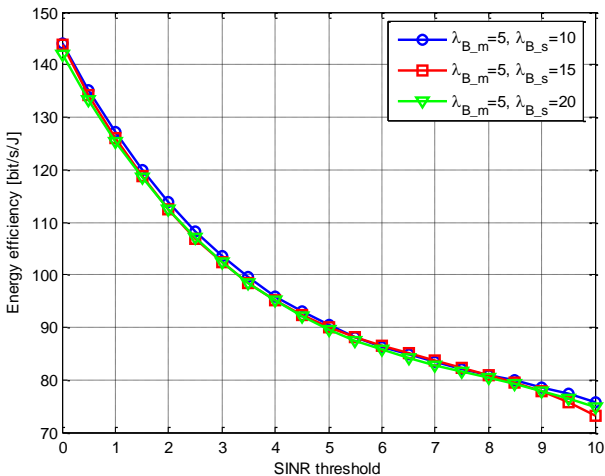


Fig. 5. Energy efficiency with respect to SBS density and SINR threshold.

impact of user mobility on the performance of UDN, and we will further extend our proposed model in the future work.

VI. ACKNOWLEDGEMENT

This work was supported by the International Science and Technology Cooperation Program of China under Grant 2015DFG12580 and Grant 2014DFA11640, in part by NFSC Major International Joint Research Project under Grant 61210002, in part by the Fundamental Research Funds for the Central Universities under Grant 2015XJGH011, in part by the EU FP7-PEOPLEIRSES, in part by project acronym S2EuNet (Grant 247083), in part by project acronym WiNDOW (Grant 318992), and in part by project acronym CROWN (Grant 610524).

REFERENCES

- [1] P. Demestichas *et al.*, “5G on the horizon: Key challenges for the radio access network,” *IEEE Veh. Technol. Mag.*, vol. 8, no. 3, pp. 47–53, Sep. 2013.
- [2] J. Andrews *et al.*, “What will 5G be?” *IEEE J. Sel. Areas Commun.*, vol. 32, no. 6, pp. 1065–1082, Jun. 2014.
- [3] X. Ge *et al.*, “User mobility evaluation for 5G small cell networks based on individual mobility model,” *IEEE J. Sel. Areas Commun.*, vol. 34, no. 3, pp. 528–541, Mar. 2016.
- [4] X. Ge *et al.*, “5G ultra-dense cellular networks,” *IEEE Wireless Commun.*, vol. 23, no. 1, pp. 1–15, Feb. 2016.
- [5] T. Zhang *et al.*, “Energy efficiency of base station deployment in ultra dense HetNets: a stochastic geometry analysis,” *IEEE Wireless Commun. Letters*, vol. 5, No. 2, pp. 184–187, Apr. 2016.
- [6] Z. Gao *et al.*, “Mmwave massive MIMO based wireless backhaul for 5G ultra-dense network,” *IEEE Wireless Commun.*, vol. 22, no. 5, pp. 13–21, Oct. 2015.
- [7] M. Renzo, “Stochastic geometry modeling and analysis of multi-tier millimeter wave cellular networks,” *IEEE Trans. Wireless Commun.*, vol. 14, no. 9, pp. 5038–5057, Sep. 2015.
- [8] M. Ding *et al.*, “Performance impact of LoS and NLoS transmissions in dense cellular networks,” in *IEEE Trans. Wireless Commun.*, vol. 15, no. 3, pp. 2365–2380, Mar. 2016.
- [9] S. Chen *et al.*, “User-centric ultra-dense networks for 5G: challenges, methodologies, and directions,” *IEEE Wireless Commun.*, vol. 23, no. 2, pp. 78–85, May. 2016.
- [10] O. Galinina *et al.*, “5G multi-RAT LTE-WiFi ultra-dense small cells: Performance dynamics, architecture, and trends,” *IEEE J. Sel. Areas Commun.*, vol. 33, no. 6, pp. 1224–1240, May. 2015.
- [11] F. Tseng *et al.*, “Ultra-dense small cell planning using cognitive radio network toward 5G,” *IEEE Wireless Commun.*, vol. 22, no. 6, pp. 76–83, Dec. 2015.
- [12] C. Yang *et al.*, “Cooperation for spectral and energy efficiency in ultra-dense small cell networks,” *IEEE Wireless Commun.*, vol. 23, no. 1, pp. 64–71, Mar. 2016.
- [13] A. Ghazanfari *et al.*, “Ambient RF energy harvesting in ultra-dense small cell networks: performance and trade-offs,” *IEEE Wireless Commun.*, vol. 23, no. 2, pp. 38–45, May. 2016.
- [14] X. Ge *et al.*, “Spatial spectrum and energy efficiency of random cellular networks,” *IEEE Trans. Commun.*, vol. 63, no. 3, pp. 1019–1030, Mar. 2015.
- [15] T. Camp *et al.*, “A Survey of Mobility Models for Ad Hoc Network Research,” *Wireless Commun. Mobile Comput.*, vol. 2, no. 5, pp. 483–502, Aug. 2002.
- [16] J. G. Andrews *et al.*, “A Tractable Approach to Coverage and Rate in Cellular Networks,” *IEEE Trans. Wireless Commun.*, vol. 59, no. 11, pp. 3122–3134, Nov. 2011.